Electroluminescence Properties of Poly(3-hexylthiophene)–Cadmium Sulfide Nanoparticles Grown *In Situ*

C. Borriello,[1] S. Masala,[1] V. Bizzarro,[2] G. Nenna,[1] M. Re,[3] E. Pesce,[3] C. Minarini,[1] T. Di Luccio[1]

[1]*Agenzia nazionale per le nuove tecnologie, l'energia e lo sviluppo economico sostenibile (ENEA), Unità Tecnica Tecnologie Portici Laboratorio Nanomateriali e dispositivi (UTTP-NANO) Centro Ricerche Portici, Piazzale E. Fermi, 80055 Portici (Napoli), Italy*
[2]*Ingegneria dei Materiali polimerici e compositi e Strutture (IMAST), Piazzale E. Fermi, 80055 Portici (Napoli), Italy*
[3]*Agenzia nazionale per le nuove tecnologie, l'energia e lo sviluppo economico sostenibile (ENEA), Unità Tecnica Tecnologie Materiali Brindisi, Laboratorio Materiali Compositi e Nanostrutturati (UTTMATB-COMP), Centro Ricerche Brindisi, SS7 Appia Km 713, 72100 Brindisi, Italy*

Received 28 April 2011; accepted 28 April 2011
DOI 10.1002/app.34774
Published online 11 August 2011 in Wiley Online Library (wileyonlinelibrary.com).

ABSTRACT: In this work, a simple approach to prepare luminescent poly(3-hexylthiophene)–CdS nanocomposites to be employed in organic light emitting devices (OLED) devices is reported. The nucleation and growth of CdS nanoparticles were obtained by the thermolysis of a single Cd and S precursor dispersed in the polymer at three different temperatures of annealing: 240, 265, and 300°C. In this way, it was possible to compare the properties of nanocomposites containing nanoparticles with different sizes. X-ray diffraction and transmission electron microscopy analyses confirmed the formation of CdS nanoparticles and gave information about the size, distribution, and morphology of the nanoparticles; monodispersive and very small nanoparticles with diameters below 2.5 nm were obtained at 240°C. The application of such nanocomposites as emitting layers in OLED devices is discussed. Enhanced electrooptical properties were observed for the device containing the nanocomposite annealed at 240°C with respect to the pure polymer based device. © 2011 Wiley Periodicals, Inc. J Appl Polym Sci 122: 3624–3629, 2011

Key words: conducting polymers; nanocomposites; nanoparticles

INTRODUCTION

Nanocomposites obtained by combining conducting polymers and semiconductor nanoparticles have so far attracted much interest for manifold applications, such as tunable luminous sources for field emission displays and electroluminescent devices.[1] Hybride nanocomposites have several advantages with respect to fully organic or fully inorganic systems.[2] As an example, polymers embedding semiconducting nanoparticles combine their good processability, high transparency, and digital printing flexibility on a large scale with the unique optical properties of the nanoparticles. To date, a wide number of different semiconductor nanoparticles with a high quantum yield and a wide luminescence band like inorganic phosphors has been developed. The size and type of nanoparticles determine the emission color.[3] In particular, the combination of II–VI semiconductor nanocrystals (or quantum dots) with conjugated polymers has been found to enhance the electroluminescence (EL) properties of these materials and to improve the long-term stability, color tunability, and quantum efficiencies of electroluminescent devices based on such nanocomposites.[3]

Nowadays, intensive research efforts have increasingly focused on the development of efficient electroluminescent hybrid nanoparticle–polymer materials for the fabrication of flexible organic light-emitting devices. One major difficulty is the control of the size, shape, and distribution of nanoparticles, which may influence the EL features. Usually, the introduction of nanoparticles within a polymer requires the use of surfactants to ensure their solubility in the conducting polymer solution. Nevertheless, the presence of surfactants and ligands on the nanoparticle surface can limit the conductivity of nanocomposites.[4] Growing nanoparticles directly in a polymer matrix has been proposed as a valid method for guaranteeing an almost uniform distribution of nanoparticles and for avoiding the use of additional surfactants.

This work shows the synthesis of conducting and luminescent hybrid nanocomposite materials by the nucleation and growth of CdS nanoparticles directly in the polymer poly(3-hexylthiophene) (P3HT). The purpose of our research was to improve the optoelectronic properties of the polymer through the enhancement of the luminescence intensity when the

Correspondence to: C. Borriello (carmela.borriello@enea.it).

polymer was sandwiched between two electrodes or through tuning the emission wavelength. CdS nanoparticles were synthesized by the thermolysis of a cadmium bis(thiolate) precursor, without the use of any surfactant or other stabilizing agents.

The size of the CdS nanoparticles was controlled by variation of the annealing conditions. The nanoparticle morphology and dimensions were investigated by X-ray diffraction (XRD) and transmission electron microscopy (TEM) analyses, whereas the optical properties were studied by ultraviolet–visible (UV–vis) absorption measurements.

The P3HT-based nanocomposites were used for the realization of a single-layer OLED device with a structure of indium tin oxide (ITO)/P3HT–CdS/Al, whose transport and emission properties were compared to the analogous pure polymer device.

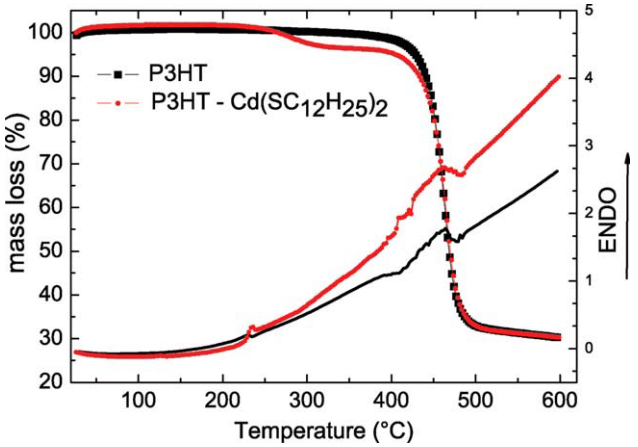

Figure 1 TGA and DSC of P3HT and P3HT–$Cd(SC_{12}H_{25})_2$. [Color figure can be viewed in the online issue, which is available at wileyonlinelibrary.com.]

EXPERIMENTAL

Reagents and characterization

P3HT (regioregular, 99%) was purchased from Sigma-Aldrich (St. Louis, MO).

Glass substrates (Corning 1737, Delta Technologies, Limited Stillwater, MN), coated with a 150 nm thick ITO layer, were used as anodes, cleaned with deionized water, detergent, and ultrasound, and dried in an oven at 115°C for 2 h. The ITO was patterned through inverse photolithography and HCl-based etching to define the anode electrode area.

Thermogravimetric analysis (TGA) and differential scanning calorimetry (DSC) were carried out in a dynamic nitrogen atmosphere from room temperature to 600°C at a heating rate of 10°C/min with a STA 449 F3 Jupiter (Netzsch, Verona, Italy).

The XRD measurements were recorded through coupled θ/2θ scans with angular steps of 0.05° and a count/step of 25 s by an X'PERT MPD (Almelo, The Netherlands).

TEM measurements were performed with a TECNAI G2 F30 (Hillsboro, OR) transmission electron microscope present at ENEA C. R. Brindisi. The samples for TEM were prepared by the dissolution of a few milligrams of annealed nanoparticle–polymer foil in a few microliters of chlorobenzene. This solution was drop-cast on Cu grids 3.05 mm in diameter and 300 mesh.

The absorption measurements in the UV–vis region were realized on films 100 nm thick deposited on a quartz substrate by a PerkinElmer Lambda 9 spectrophotometer (Waltham, MA).

The EL analysis was performed with a Newport 810UV photodiode connected to a Keithley 6517A electrometer (Cleveland, OH).

The current–voltage characteristics of the devices were measured in dark conditions at room temperature with a Keithley 2400 power supply source meter in voltage mode in the range 0–10 V with constant increment steps and a delay time of 1 s before each measurement point.

Synthesis of the nanocomposites and device preparation

The method used to synthesize the nanocomposites was reported in a previous work[5] with some modification.

Cadmium dodecanethiolate [$Cd(SC_{12}H_{25})_2$] was used as a Cd and S precursor. The polymer P3HT was dissolved in chlorobenzene at a concentration of 25 mg/mL. The precursor was successively added to this solution at 20 wt %. A bulk foil was obtained by casting and annealed at 240, 265, and 300°C *in vacuo*.

To realize the OLED device structure, the nanocomposite solution was spin-coated (2000 rpm) on a patterned ITO/glass substrate used as an anode electrode. The Al cathode electrode (100 nm thick) was deposited by thermal evaporation through a shadow mask.

RESULTS AND DISCUSSION

Previous studies on the nucleation and growth of CdS nanoparticles by thermolysis have shown that the formation of the nanoparticles starts at temperatures of about 170°C in a thermoplastic copolymer.[5] However, the choice of the annealing temperatures depends also on the decomposition temperature of the CdS precursor in the matrix and on the melting and decomposition temperatures of the polymers. A thermal analysis was conducted by TGA and DSC on the polymer and the bulk P3HT–$Cd(SC_{12}H_{24})_2$ (Fig. 1).

The TGA measurement showed that the precursor mass loss started around 220°C and was complete at

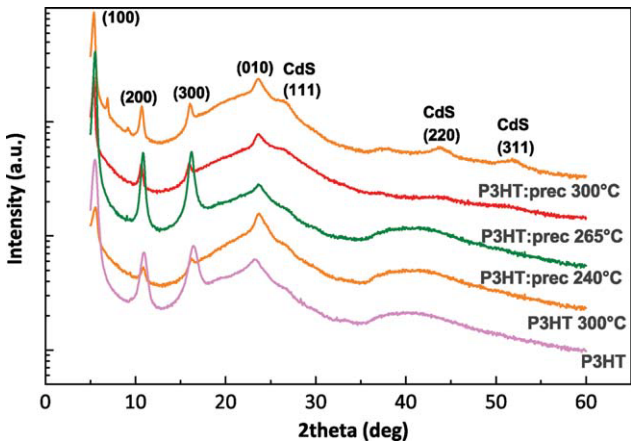

Figure 2 XRD analysis of P3HT–CdS nanocomposites obtained at 240, 265, and 300°C, P3HT as prepared and annealed at 300°C. [Color figure can be viewed in the online issue, which is available at wileyonlinelibrary.com.]

about 300°C, whereas P3HT had the peculiarity to start its degradation at high temperatures, above 400°C. The DSC analysis exhibited an exothermic peak at 228°C, the attributed melting point of P3HT. For these reasons, annealing in P3HT was carried out at 240, 265, and 300°C. In this way, it was possible to compare the behavior of nanocomposites containing nanoparticles with different sizes and size distributions.

XRD analyses confirmed the formation of CdS nanoparticles. In Figure 2, we compare the XRD data of the P3HT–CdS nanocomposites after annealing at 240, 265, and 300°C and P3HT, both as-prepared and after annealing at 300°C. The spectrum of the P3HT–CdS nanocomposite annealed at 240°C was very similar to the spectrum of P3HT that was not annealed. The Bragg peaks of P3HT, (100), (200), (300), and (010), and the CdS ones were indexed,. The large amorphous background underneath the P3HT (010) reflection came from the glass slide used to hold the polymer foil during the XRD experiment. The CdS nanoparticle signal was not yet visible at 240°C because, at this temperature, the nanoparticles were too small and the number density was low. The diffraction features changed when the annealing temperature was raised to 265°C. Here, the crystalline reflections from the CdS nanoparticles became visible. They corresponded to the (111), (200), and (220) peaks of the CdS cubic phase. Correspondingly, the intensity of the P3HT crystalline peaks decreased after annealing above 240°C. The nanoparticle dimension was estimated to be about 5 nm for the sample annealed at 300°C.

TEM images (Fig. 3) taken at low magnification showed spherical and very small nanoparticles, mainly grouped in some areas where the polymer filaments were present. The high-resolution TEM images indicated the formation of nanoparticles characterized by a spherical shape and regular lattice fringes at distance of 0.31 nm in all of the samples. We determined the average diameter of nanoparticles by a statistical analysis on several low-magnification pictures of the samples. From such analysis, we deduced that the relatively low temperature favored the nucleation of nanoparticles and their growth up to about 2 nm in diameter. Higher temperatures promoted an increase in the average size, from 2.5 nm at 240°C to 3 nm at 265°C and 4.5 nm at 300°C, but caused a reduction in the mean distance between the particles (Fig. 3).

UV–vis spectra of the P3HT and P3HT–CdS nanocomposites are reported in Figure 4. A strong absorption band was observed at 507 nm due to the excitation of electrons in the π-conjugated polymer.[6] The shoulder at higher wavelength was due to interchain interaction in the polymer.[7] The presence of CdS nanoparticles could not be detected with a specific peak in the absorption spectra of Figure 4. The absorption of a nanocomposite may not be simply the sum of the two components (nanoparticles + polymer), as reported by other groups.[8] Thus, the most visible effect of the CdS nanoparticles was the increase of the absorption signal in the range 250–400 nm. Such changes in the absorption curves could not be ascribed to modification or ordering of the polymer chains induced by the annealing process because the absorption spectra of pristine P3HT and P3HT annealed were similar (not reported in the figure). On the other hand, it is worth noting that the absorption increase in the UV region in our case was less pronounced than in Verma and Dutta[8] because of the low nanoparticle concentration with respect to P3HT. Such a hypothesis was confirmed by a comparison between the UV–vis absorption measured on commercial 2–3 nm CdS nanoparticles (purchased by NN-Labs, Fayetteville, AR) dispersed in P3HT at a concentration of 20 wt % and P3HT only (inset of Fig. 4). The experiment was performed in solution. The signal due to the CdS nanoparticles was weak but visible above the P3HT signal and is indicated by the gray arrow in Figure 4. In our case, the CdS concentration with respect to P3HT was much lower. From the initial 20% wt of precursor with respect to P3HT, we can estimate a theoretical yield of 4 wt % of nanoparticles.

The P3HT–CdS nanocomposites were employed to prepare simple OLED devices with the structure ITO/P3HT–CdS/Al. The experimental measurements (Fig. 5) were performed with the devices under testing kept at a constant current (10 mA). The EL of the devices based on the nanocomposites annealed at 240 and 265°C was enhanced with respect to the one of P3HT, whereas at 300°C, a strong reduction of the EL was observed.

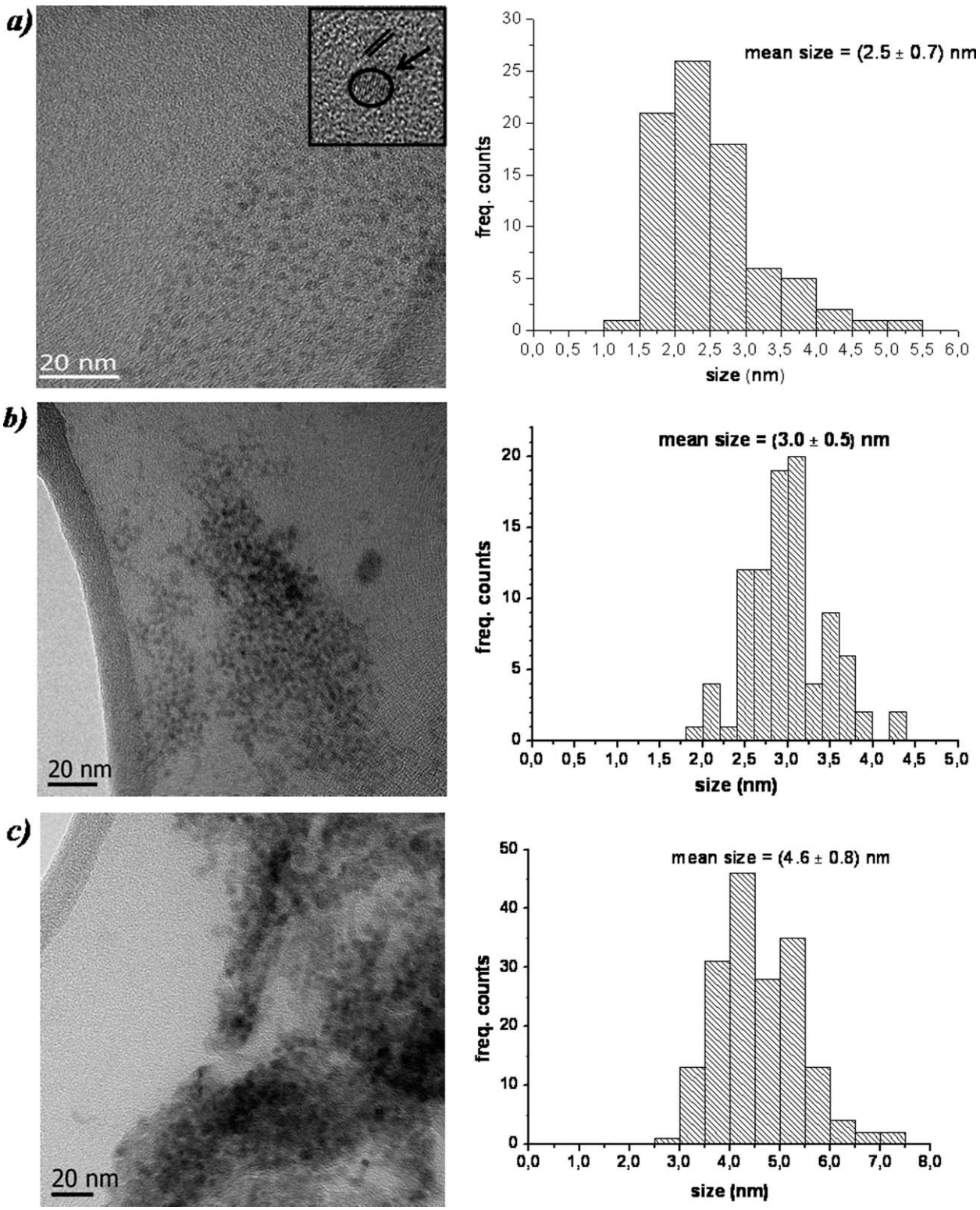

Figure 3 Bright-field TEM image of CdS nanocrystals in the P3HT matrix and statistical distribution of the nanoparticle size evaluated from a sampling of about 100 nanoparticles after annealing at (a) 240, (b) 265, and (c) 300°C.

The rise in the EL signal may suggest an effect of the energy-transfer mechanism, in particular, Förster energy transfer, which consists of an exciton transfer between the two materials of the composite.[9] This effect is usually reported for energy transfer from a matrix to a dye material,[4,10,11] whereas few studies have reported on the energy transfer from the nanoparticles to polymers or dyes.[12,13] On the other hand, in our case, the exciton should have transferred from CdS nanoparticles to the polymer

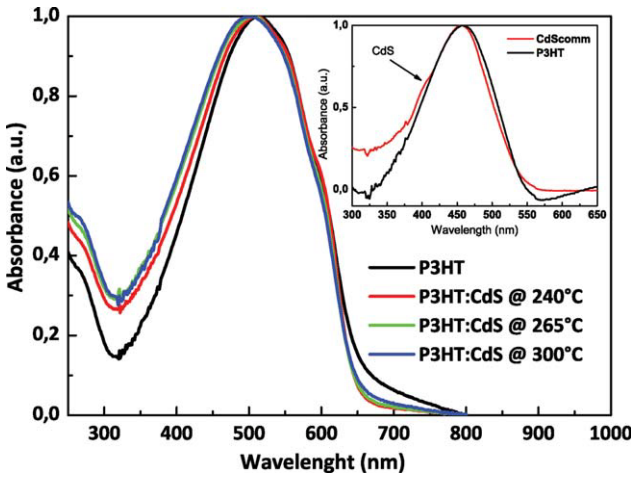

Figure 4 UV–vis spectra of P3HT and P3HT–CdS nanocomposite solutions synthesized at 240, 265, and 300°C. The inset shows the absorption of commercial CdS nanoparticles (size = 2–3 nm) dispersed in P3HT and P3HT only. [Color figure can be viewed in the online issue, which is available at wileyonlinelibrary.com.]

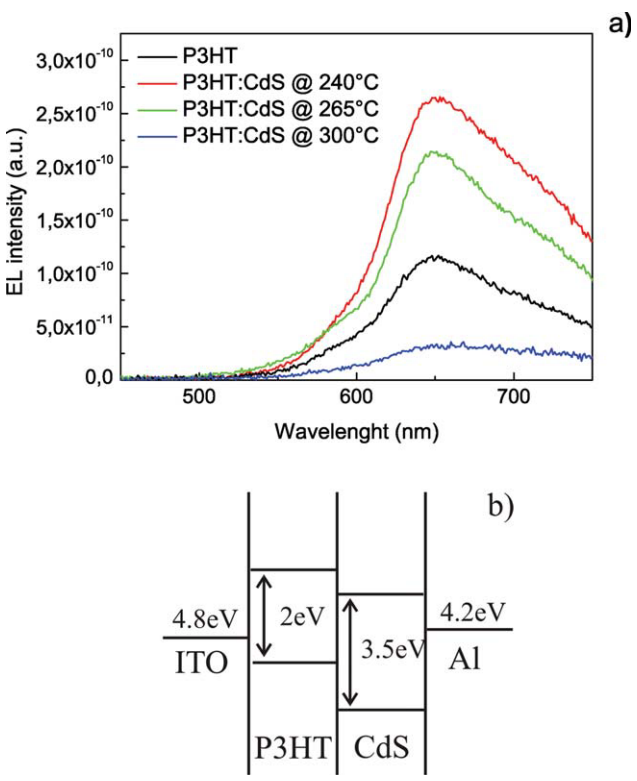

Figure 5 (a) EL spectrum of ITO/P3HT/Al and ITO/P3HT–CdS/Al synthesized at 240, 265, and 300°C and (b) energy level diagram of the ITO/P3HT–CdS/Al device. As discussed in the text, the energy gaps were derived from the literature for P3HT[2,14] and from the UV–vis absorption of CdS synthesized in a transparent polymer.[16] [Color figure can be viewed in the online issue, which is available at wileyonlinelibrary.com.]

because of the larger energy gap of CdS respect to P3HT.[4] In principle, the Förster energy-transfer process was possible because the photoluminescence of CdS nanoparticles grown in the transparent polymer topas at temperatures between 230 and 250°C overlapped with the absorption of P3HT.[5] The energy transfer mechanism could be qualitatively described by the band diagram, shown in Figure 5(b). The exact energy levels of the single materials were not precisely known. Therefore, for P3HT, we used an average value from the literature (lowest unoccupied molecular orbital = 3 eV and highest occupied molecular orbital = 5.1 eV),[2,14] whereas for CdS, we used the values conduction band (CB) = 3.8 eV and valence band (VB) = 7.2 eV, evaluated from the known electron affinity of CdS of 3.8eV[15] and the energy gap of 3.5 eV, measured by the UV–vis absorption of CdS nanoparticles synthesized in topas, where the nanoparticle signal was clear.[16]

The optimal EL properties were found in the nanocomposite annealed at 240°C and containing the smallest nanoparticles. On the other hand, the increase of nanoparticle size with annealing temperature produced a redshift of the emission spectrum of the CdS nanoparticles[5] that may have limited the energy transfer process and reduced the device efficiency. An important role in the overall process was also played by the thiol chains coming from the precursor. In fact, at low temperature, the presence of residual thiol chains from the decomposition process ensured a homogeneous distribution of the particles in the matrix [Fig. 3(a)]. At higher annealing temperatures, the almost complete decomposition of the precursor led to the agglomeration of nanoparticles, as is clearly visible in Figure 3(c). The lack of ligands around the nanoparticles favored the charge transfer

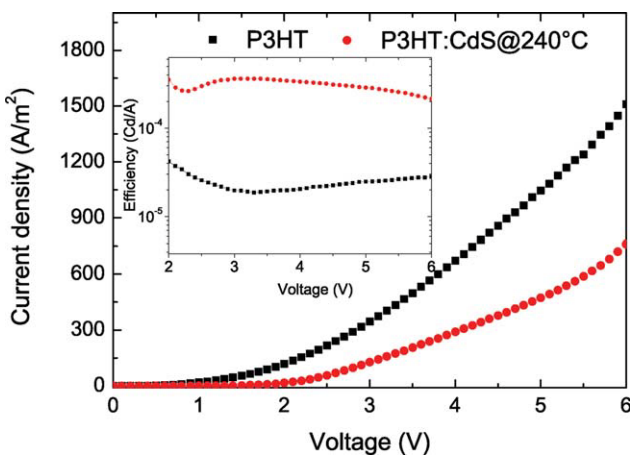

Figure 6 Current density–voltage characteristics and efficiency (inset) as a function of voltage of the devices ITO/P3HT/Al and ITO/P3HT–CdS/Al annealed at 240°C. [Color figure can be viewed in the online issue, which is available at wileyonlinelibrary.com.]

more than the exciton transfer[4] and reduced the radiative recombination of the charge carriers.[17]

The current–voltage characteristics of the device, including the nanoparticles annealed at 240°C, and compared with the device of P3HT only are reported in Figure 6. The turn-on voltages of P3HT–CdS after annealing shifted to higher values, and the current density decreased with respect to the P3HT test device. This result may, again, be attributed to the presence of the residual thiol chains, which acted as an insulating layer around the nanoparticles and reduced the conductivity of the nanocomposite. The inset of Figure 6 shows that the external efficiency (in units of Cd/A) was increased by the presence of the nanoparticles by one order of magnitude. The low absolute values of the efficiency found in the devices could be improved by the introduction of injection layers and blocking layers between the active layer and the contacts to favor the charge injection and the exciton confinement, respectively. However, the electrooptical properties of the devices might also have been influenced by roughness at the Al interfaces caused by the partial penetration of Al in the underneath nanocomposite.[18] Such inhomogeneities could be the source of undesired current paths. A good solution to avoid Al penetration would be the deposition of a thin protective layer (LiF, MgO) between the Al electrode and the nanocomposite layer to improve the electron injection.

CONCLUSIONS

Luminescent P3HT nanocomposites containing CdS nanoparticles were synthesized by *in situ* thermolysis of a cadmium dodecyl thiolate. The CdS nanoparticle size and distribution were controlled by variation of the annealing temperature between 240 and 300°C. The nanoparticles obtained were very small (from 2.5 to 4.6 nm) and showed a narrow size distribution in the polymer, as indicated by TEM analysis. This synthetic approach allowed the use of a single, air-stable, and easy-to-prepare precursor for both Cd and S. Moreover, the nucleation and growth of the nanoparticles directly in the polymer let us avoid the use of surfactants.

The three P3HT–CdS nanocomposites were used as an active layer of simple OLED stacks: ITO/P3HT–CdS/Al. The electrooptical properties were measured and studied for the three devices. Improved performances, in terms of spectral coverage and intensity of the emission signal with respect to pure P3HT, were obtained by the dispersion in the matrix of the smallest nanoparticles.

The authors acknowledge A. M. Laera from ENEA and Centro Ricerche Brindisi for providing the precursor.

References

1. Shipway, N.; Katz, E.; Willner, I. ChemPhysChem; Wiley-VCH-Verlag: Weinheim, 2000; Chapter 1, p 18.
2. Saunders, B. R.; Turner, M. L. Adv Colloid Interface Sci 2008, 138, 1.
3. Coe-Sullivan, S.; Woo, W. K.; Steckel, J. S.; Bawendi, M.; Bulovic, V. Org Electron 2003, 4, 123.
4. Greenham, N. C.; Peng, X.; Alivisatos, A. P. Phys Rev B 2006, 54, 17628.
5. Di Luccio, T.; Laera, A. M.; Tapfer, L.; Kempter, S.; Kraus, R.; Nickel, B. J Phys Chem B 2006, 110, 12603.
6. Inoue, K.; Ulbricht, R.; Madakasira, P. C.; Sampson, W. M.; Lee, S.; Gutierrez, J.; Ferraris, J.; Zakhidov, A. A. Synth Met 2005, 154, 41.
7. Brown, P. J.; Thomas, D. S.; Kohler, A.; Wilson, J. S.; Kim, J. S.; Ramsdale, C. M.; Sirringhaus, H.; Friend, R. H. Phys Rev B 2003, 67, 64203.
8. Verma, D.; Dutta, V. J Renewable Sustainable Energy 2009, 1, 0231.
9. Baldo, M. A.; Forrest, S. R. Phys Rev B 2000, 62, 10958.
10. Kaufmann, S.; Stoferle, T.; Moll, N.; Mahrt, R. F.; Scherf, U.; Tsami, A.; Talapin, D. V.; Murray, C. B. Appl Phys Lett 2007, 90, 071108.
11. Lutich, A. A.; Jiang, G.; Susha, A. S.; Rogach, A. L.; Stefani, F. D.; Feldmann, J. Nano Lett 2009, 2636.
12. Chowdhury, P. S.; Sen, P.; Patra, A. Chem Phys Lett 2005, 413, 311.
13. Firth, A. V.; Haggata, S. W.; Khanna, P. K.; Williams, S. J.; Allen, J. W.; Magennis, S. W.; Samuel, I. D. W.; Cole-Hamilton, D. J. J Lumin 2004, 109, 163.
14. Cook, S.; Furube, A.; Katoh, R. Energy Environ Sci 2008, 1, 294.
15. Ghezzi, C.; Paorici, C.; Pelosi, C. Appl Phys 1976, 11, 4.
16. Masala, S. Ph.D. Thesis, University of Milano-Bicocca, 2010.
17. Santhi, S.; Bernstein, E.; Paille, F. J Lumin 2006, 117, 101.
18. Masala, S.; Del Gobbo, S.; Borriello, C.; Bizzarro, V.; La Ferrara, V.; Minarini, C.; De Crescenzi, M.; Di Luccio, T. Presented at Nano 2010, Sept 2010, Rome.